ORIGINAL ARTICLE

Optical characteristics on practical verification for pico-laser-engraved glass light guide plate with concave microstructures

Tun-Chien Teng[1] · Tien-Li Chang[1] 🄬 · Hung-Cheng Tsai[1]

Abstract

Recent increasing interest in light guide plates (LGPs) based on the advanced manufacturing towards optoelectronics applications has emerged as a potential technology. The aim of this study was to estimate the optical characteristics on practical verification of laser-engraved glass light guide plate with concave microstructures. The case study can use the industrial ability of picosecond laser (pico-laser) technique, a type of ultrafast laser pulses, to directly engrave a glass sheet (Corning Iris® Glass) with functional concave microstructures for fabricating an LGP. Eight small pieces of samples with array of microstructures engraved on different processing conditions were made for measuring optical characteristics before and after the samples were etched by hydrofluoric acid. Here, the engraved 6-inch LGP structures can make light exit from the LGP uniformly. Additionally, the two optimized LGPs were put in a 7.8-inch backlight module where the measured results showed the uniformity of spatial luminance was 0.9. The study demonstrated the one-step process utilizing pico-laser technique, yielding for the design of microstructures of thinner large-sized liquid crystal display (LCD) products in the manufacturing of LGPs for lighted-up in a backlight unit (BLU).

Keywords Optical characteristics · Laser engraving · Picosecond laser technique · Glass concave microstructures · Light guide plates · Backlight

1 Introduction

Growing popularity of the thin-film-transistor liquid crystal display (TFT-LCD) has dominated the display market for all applications of various sizes. Especially for LCD TV with the size going larger and even beyond 65 inches, it consumes most production capacity of LCD and accounts for most market share. The LCD TV is mainly composed of two parts, a LC panel and a backlight unit (BLU). The edge-lit BLU become the mainstream because of the advantages of very slim volume and light-weight. Although the organic light-emitting diode (OLED) displays recently grow rapidly and challenge LCDs in all applications, they will still coexist for a long time with ongoing competition between them because each technology has its own pros and cons [1]. Therefore, researches on LCD for providing larger size, lower cost, better display quality, and higher energy efficiency should take

into consideration. Among the studies on many designs, the light guide plates (LGPs) have been the crucial component in the edge-lit BLU for efficiently providing illumination with both luminance and chromaticity uniformity in various ways [2–5]. Polymethyl methacrylate (PMMA) seems to be the most attractive one for preparing LGP structures due to its excellent optical properties with low cost. However, the plastic LGPs have specifically disadvantages such as lower stiffness, deformation by humidity, higher thermal expansion, and lower chemical and thermal stability. With the large-sized, ultra-slim LCD TV becoming more popular, the LGPs can be thinned and the supporting components in BLU are removed for further reducing the entire thickness, which leads the LGPs made of PMMA too weak to support the BLU. To address the issue, the LGPs made of glass material have been proposed. As compared with the plastic LGP, the glass LGPs can be of higher bending stiffness and lower thermal and little moisture expansion. Accordingly, the glass LGPs itself can be a body of LCD TV with no need of additional supporting components, which makes the LCD TV feature ultra-slim and light-weight [6–8].

✉ Tien-Li Chang
tlchang@ntnu.edu.tw

[1] Department of Mechatronic Engineering, National Taiwan Normal University, Taipei, Taiwan, Republic of China

In the past decides, varieties of methods for forming microstructures on the surface of plastic LGPs, including the screen-printing [9, 10], powder blasting [10], ink-jet [11], and laser engraving processes [12, 13], have been studied by being feasible for the large-sized plastic LGPs. In generally, the laser-engraving process can engrave the surface of plastic LGPs directly to form the concave microstructures in various shapes, in which the process can be no need of consumables, and rapidly print the designed or revised pattern on the bare plastic LGPs. The advantages of laser engraving technique include single-step patterning, non-contact patterning, mask-free patterning, and eco-friendly processes [14, 15]. However, if the laser engraving process is applied to the glass substrate, it will encounter the problems of mechanical durability, reusability, and smooth surface on account of the limitation on brittleness of glass [16–18]. The conventional lasers (continuous-wave and long-pulsed lasers) are not suitable for directly forming microstructures on the glass LGPs, because the effect on the mechanical and thermal deformation through the laser pulses leads to fracture occurring [19–21]. Therefore, currently screen-printing is used for forming paint dots on the surface of glass LGP. In contrast to conventional laser, the ultrafast laser (femtosecond or picosecond laser) technique has been recently applied to the micromachining of microstructures in glass due to the advantages associated with the nonlinear process with optical breakdown and plasm, while the high beam intensity (pulse energy) on the order of 10^{13}–10^{14} W/cm^2 can be focused within the point of a material [22–24]. The ultrafast laser with short pulse duration has the characteristics of multiple-photon absorption and minimize heat-affected zone (HAZ) whose nonlinear process at the focus spot can be suitable for removing the surface glass material [25–28].

Very recently, Ito et al. [29] reported the formation of damage based on the controlled pulses in femtosecond laser drilling on chemically strengthened glass substrate. Although many studies of ultrafast laser techniques in glass were expended in using the simulation methods, and the experimental observation of morphologies of micro- and nano-structures [26–31], engraving glass LGP techniques are lacking primarily due to the fact that the required results under the design of experimental arrangements must be done in backlighting application. For the presence domain, only few studies have carried out the possible interactions between ultrafast laser and glass LGP surface techniques. In this study, one-step ultrafast laser treatment can significantly provide an effective means to engrave the surface of brittle glass LGPs for backlighting.

In this paper, we present the results of the glass LGP surface study through the industrial ability of 532-nm pico-laser technique to directly engrave the glass sheet (Corning Iris® Glass) with concave microstructures under ambient atmosphere. The purpose of this study is to provide an estimate of the optical characteristics on practical verification of laser-engraved glass LGP with concave microstructures at the different the types of laser-ablated path. The study demonstrates the feasibility of the method by fabricating a required LGP sample of size up to 140 mm × 70 mm for being lighted-up in a BLU.

2 Experimental

2.1 Pico-laser engraving system

The experiments for engraving concave microstructures in air were performed using a visible light ultrafast laser, based on a picosecond laser system (Advanced Optowave Corp., model: ALTA-PS-532 W, USA), producing pulses of 7 ± 2 ps duration at a wavelength of 532 nm with repetition rate 300 kHz. The scanner control application software was used to control all laser engraving routines. The experimental laser setup and process of directly engraving 6-inch glass sheet (Corning Iris® Glass) into functional concave microstructures for LGPs was presented in Fig. 1. The dimensions of the used LGPs were 140 mm(length) × 70 mm(length) × 2 mm(thickness). The transverse mode of the laser was TEM_{00}, and the beam quality factor (M^2) was less than 1.3. An optical scanner (three-dimensional laser scan system) with high-precision XY sample scanning stages was used to steer the laser beam to scan across the substrate surface with a predetermined engraved structures.

2.2 Fabrication and measurement

To fabricate the required concave microstructures, the types of laser-ablated path were used for point processing and line-scan (line-direction scanning) processing to engrave the surface structure in glass, as shown in Fig. 2(a)–(b). The formed microstructures determined the focusing distance (FD) during laser processing, as shown in Fig. 2(c). In this study, the focal distance can be removed the material where the needed ablation occurs, the positive focal distance while the focus of the laser beam moving upward from zero point, and the negative focal distance while the focus of the laser beam moving downward from the zero point. The point processing was used for engraving tiny shallow pits on the surface of the glass; the line-scan processing was used for engraving grooved microstructures on the surface of the glass. In general, the slopes of the profile of the tiny shallow pit are small and vary smooth, but the slopes of the profile of the grooved microstructure are steep and vary abruptly, in which the light hitting the grooved microstructures will angularly diffuse more obviously than the

Fig. 1 Schematic of picosecond laser system setup for engraving glass LGPs
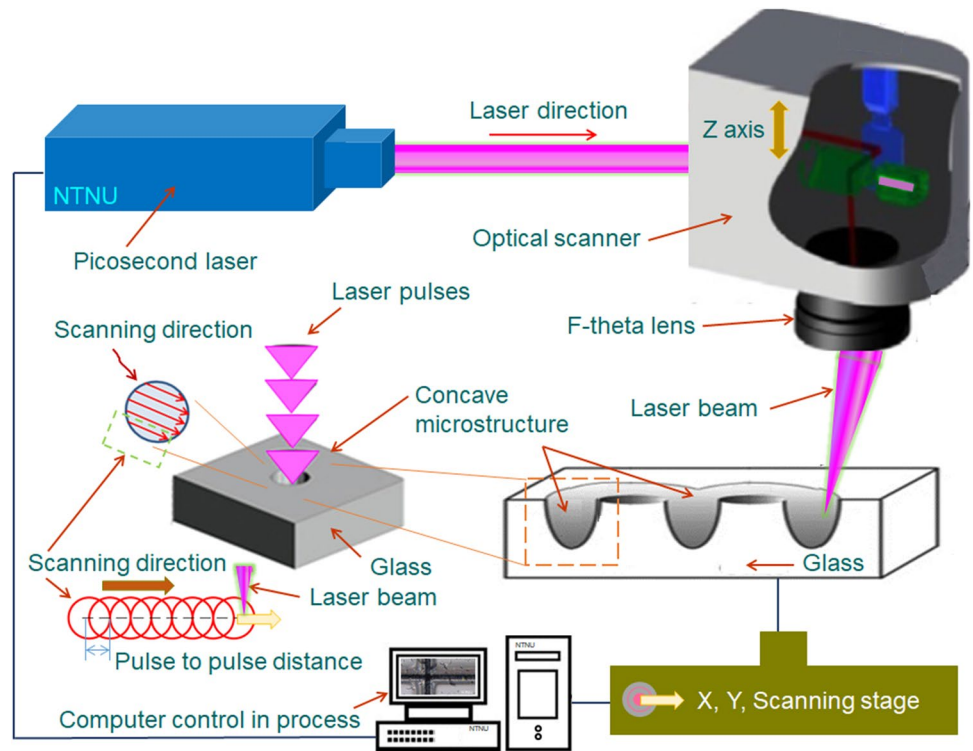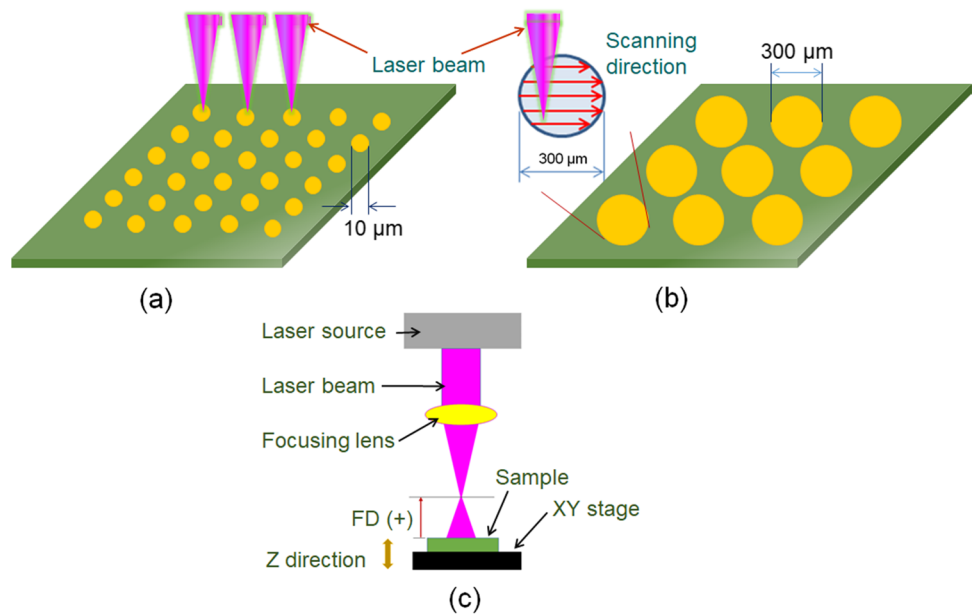

Fig. 2 Schematic of laser-ablated path showing (a) point and (b) line-scan processing to engrave the surface structure in glass. (c) The formed microstructures determined the focusing distance (FD) during laser processing

light hitting the shallow pits. Therefore, the two types of the microstructures make the light emerging from the LGP have different optical behaviors. In the discussion section, the preliminary results of the experiment were analyzed. First, the process windows were determined for engraving concave microstructures by point processing and line-scan processing, respectively. According to the process windows, the optimal process conditions were

obtained. Second, three types of glass samples with different microstructures were fabricated under the optimal conditions, and then were etched by hydrofluoric acid (HF) to smooth the surfaces of the engraved microstructures and removed debris for investigating its effect on microstructures' profile. Third, eight types of samples with different microstructures were fabricated for investigating the optical characteristics before and after they

were etched. Fourth, a 6-inch sample of the glass LGP with engraved microstructures was fabricated and lighted-up in a BLU for measuring the optical performance.

Among the above stages, the width and the depth of the microstructures on the samples engraved under different conditions were measured by a laser-scanning confocal microscope (LSCM, OLS4000, Olympus Corporation, Japan) and a scanning electron microscope (SEM, JSM-7610F, JEOL Ltd., Japan). Moreover, a conoscope (Autronic Melchers GmbH, German) and a luminance meter (BM7A, Topcon Corporation, Japan) were used to measure the angular intensity and the spatial luminance of the samples edge-lit by an LED light-bar.

3 Results and discussion

3.1 Effect of laser pulses on point processing

The process windows were determined for engraving concave microstructures by point processing in the first stage. The engraving time for the point processing was 0.01 ms; the repetition rate of laser pulse for both the processing was 300 kHz. Figure 3 indicates that the width and depth of the microstructures (pit) engraved by point processing varies with the focus at the laser output powers of 3 W, 3.5 W, and 4 W. With the engraving time of 0.01 ms at a repetition rate of 300 kHz for processing each microstructure, the output power of 3.5 W and 4 W had relatively lower variation in the widths and depths within a focal range of 0.53 mm, while the focal range of 3 W was narrow. Because the glass used for fabricating the LGP was highly transparent for the visible light, the effect of the ablation of the 532-nm laser on the glass was sensitive to the focus. When the focal position was away from the optimal position, the effect of the

ablation dramatically dropped such that both the depth and the width of the engraved pits decreased. With considering the maximal output power of the laser machine of 4.3 W, we preferred 3.5 W to ensure the stable output power of the laser. Next, we investigated the effect of the engraving time (ET) at a repetition rate of 300 kHz on the microstructure's appearance at the focusing distance of 0 mm and the power of 3.5 W; the results are shown in Figs. 4 and 5. Figure 4 indicates that the width and depth of the pits substantially increased with the engraving time because of ablation accumulating. However, the width trended to saturation with the engraving time over 0.05 ms. Thus, the aspect ratio of the pits increased with the engraving time. Figure 5 indicates that the crater-like profile became more obvious as the engraving time over 0.03 ms because the ablated material recast and accumulated around the pits. Therefore, the user-define crater-like structures on the glass surface can be formed by increasing the engraving time. Either increasing the aspect ratio or forming crater-like structure aids the pits in extracting the light from the LGP. In addition, the accumulated debris around the pit affected the measurement accuracy of the width of the pit, which caused the variation of the width in the saturation region as shown in Fig. 4.

3.2 Effect of laser pulses on line-scan processing

The process windows were also determined for engraving concave microstructures by line-scan processing in the first stage. The concave microstructure engraved by line-scan processing was bounded by an engraved circle line of a 300 μm diameter, so the diameters of the concave microstructures substantially kept the same for all the conditions. The results are shown in Fig. 6 and indicate that the depth of the microstructures engraved by line-scan processing varies with the focus at the laser output powers of 3 W, 3.5 W, and

Fig. 3 Process window for the pits engraved by point processing: width vs focus; depth vs focus
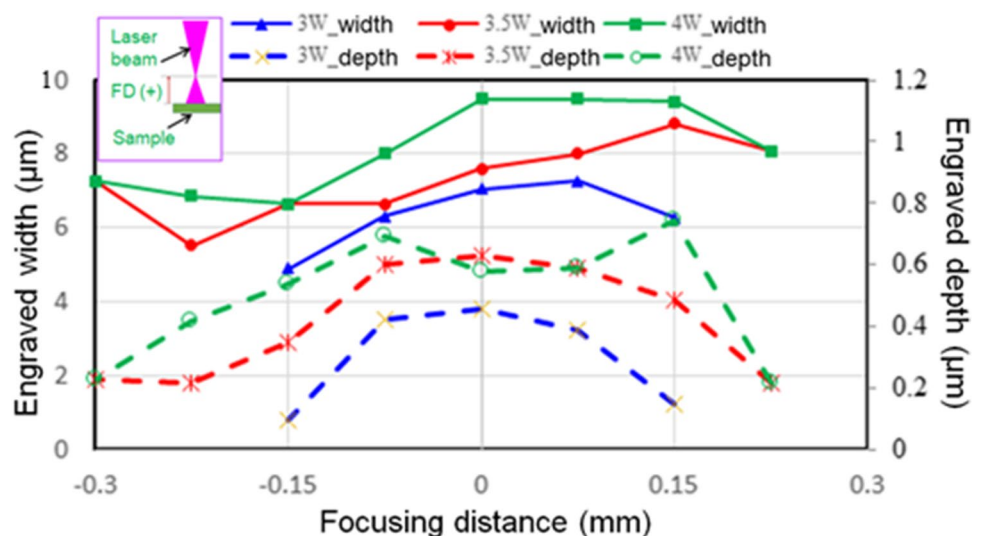
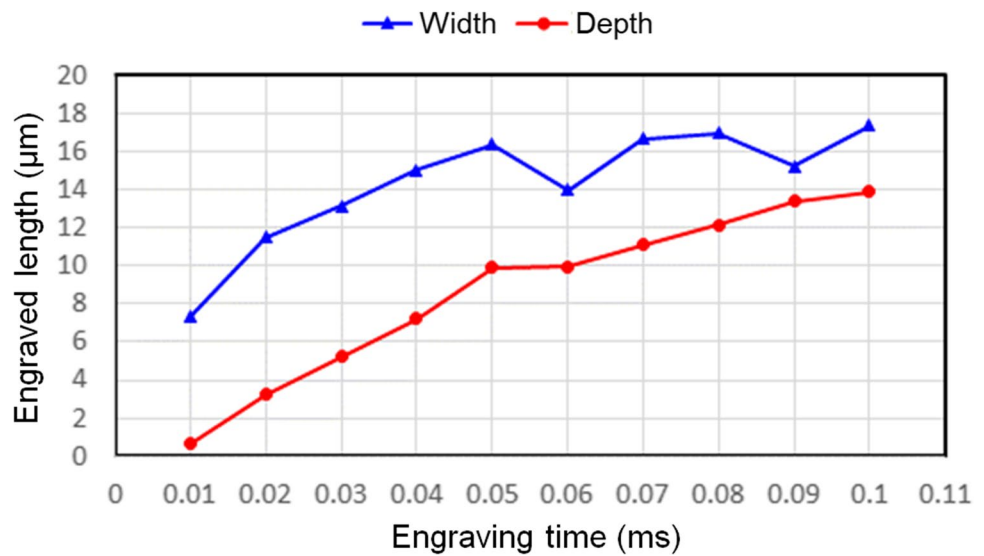**Fig. 4** The depth and width of the pits for various engraving time at the focus of 0 mm and the power of 3.5 W

Fig. 5 The appearance of pits engraved by point processing for various engraving time at the focus of 0 mm and the output power of 3.5 W
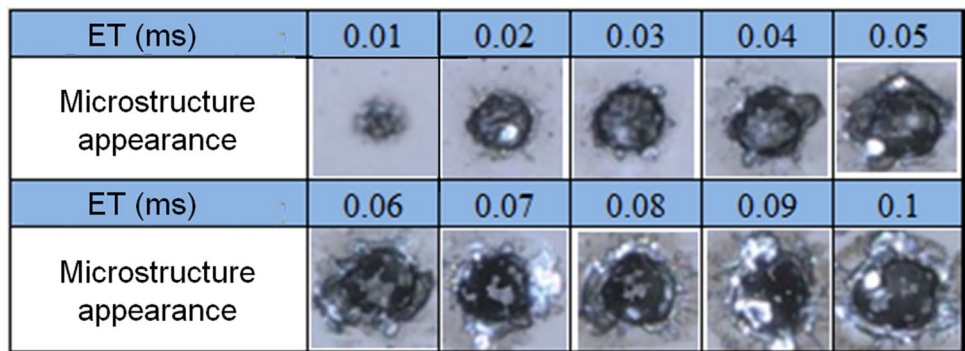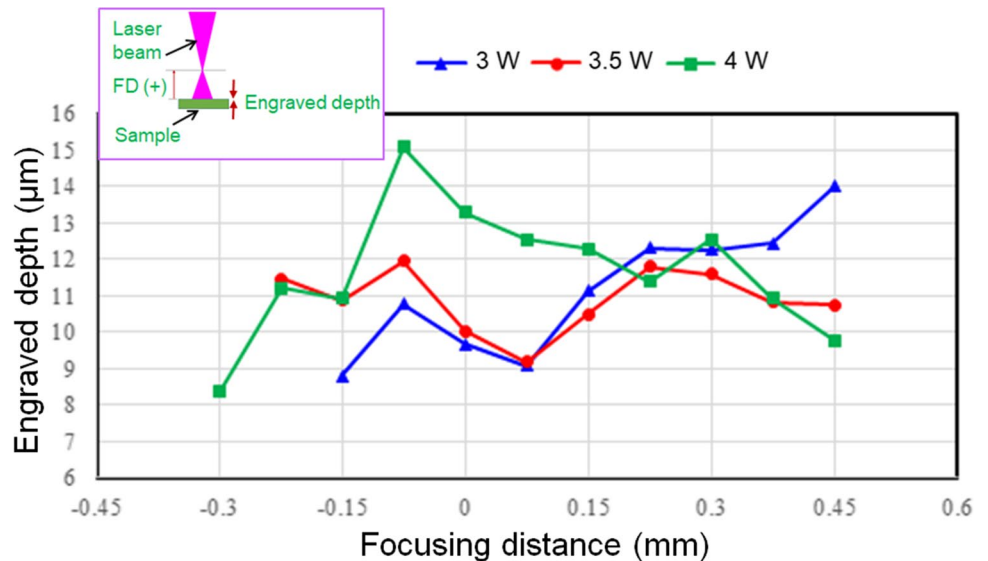

ET (ms)	0.01	0.02	0.03	0.04	0.05
Microstructure appearance					
ET (ms)	0.06	0.07	0.08	0.09	0.1
Microstructure appearance					

Fig. 6 Process window for the microstructures engraved by line-scan processing: depth vs focus

4 W. The output power of 3.5 W had smallest variation in the depths and maintained good appearance within a focal range of 0.68 mm (as shown Fig. 7), so we chose 3.5 W and 0.12 mm as the optimal values of the output power and focusing distance (FD), respectively. Because the ratio of shot overlapping was 98.9% in the line-scan processing, the

depth of the engraved microstructure was much deeper than the pit engraved by the point processing. In addition, the focal range of the line-scan processing was wider than the point processing.

Next, we investigated the effect of the engraving rounds on the depth and width of the grooves in the microstructures engraved by line-scan processing at the focusing distance of 0.12 mm and the power of 3.5 W. The results are shown in Fig. 8 and indicate that the depth and width of the grooves substantially increased with the number of engraving process (N, engraving rounds). Considering the depth and processing time, we chose 3 engraving rounds as the optimal values. Then, we checked the effect of the scan-pitch on the appearance of the microstructures engraved by 3 rounds at

the focus of 0.12 mm and the power of 3.5 W. The results indicated that the smaller scanning pitch (SP) distance made the grooves in the microstructure overlap and disappear, as shown in Fig. 9.

3.3 Effect of HF etching on engraved microstructures

To smooth the surfaces, the engraved microstructures and removed debris can be used by HF etching. In the experiment, the samples were made by engraving a glass sheet with three types of array of the concave microstructures under the optimal conditions at a repetition rate of 300 kHz using the output power of 3.5 W, including the pits with an array pitch

Fig. 7 The appearance of microstructures engraved by line-scan processing at various focuses with the output power of 3.5 W

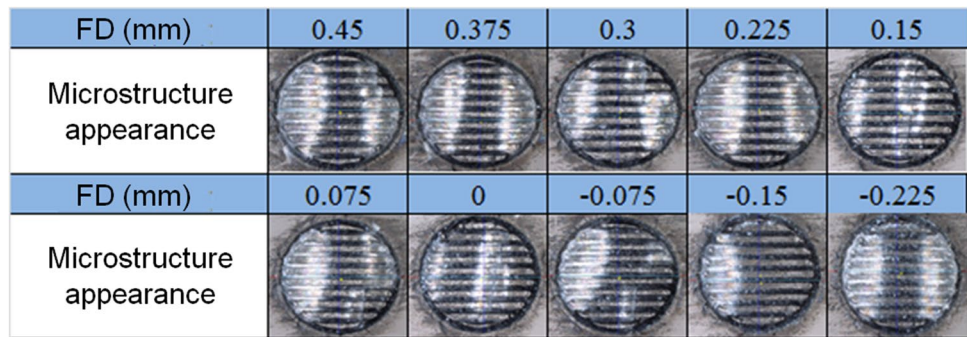| FD (mm)	0.45	0.375	0.3	0.225	0.15
Microstructure appearance					
FD (mm)	0.075	0	-0.075	-0.15	-0.225
Microstructure appearance					

Fig. 8 The depth and width of the grooves in the microstructures engraved for various times of line-scan processing at the focus of 0.12 mm and the power of 3.5 W
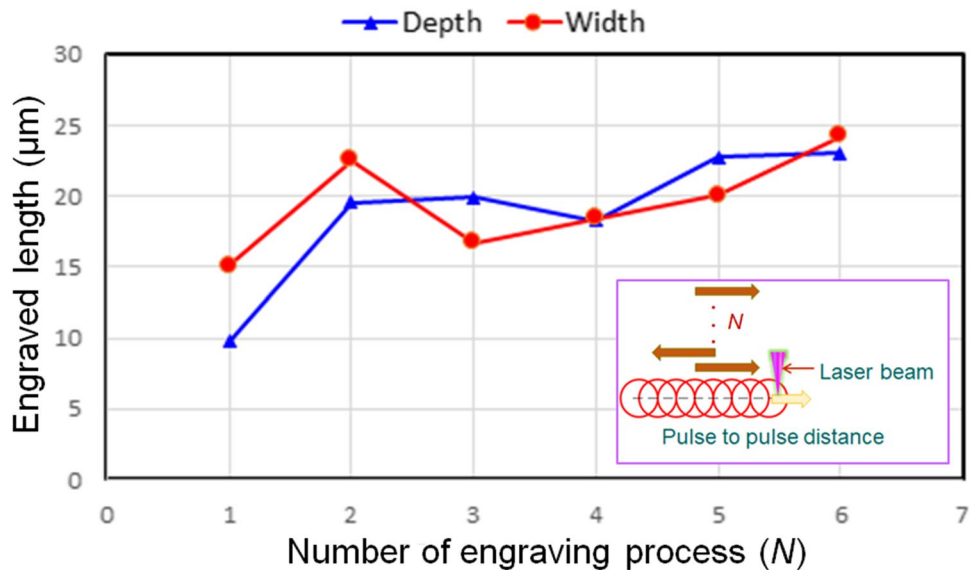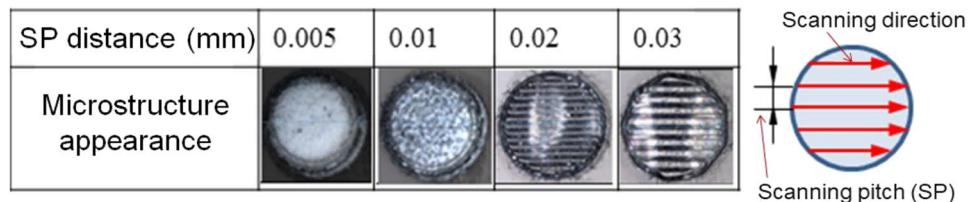

Fig. 9 The effect of SP distance on the appearance of the microstructures

SP distance (mm)	0.005	0.01	0.02	0.03
Microstructure appearance				

of 0.05 mm and the engraving time of 0.01 ms (case A), the line-scan microstructures with an array pitch of 1 mm, and scan-pitches of 0.01 mm (case B) and 0.03 mm (case C). The samples were etched by the HF etchant (DI water containing HF of 5 wt%) for a period of 10 min, 20 min, and 30 min. Then, we investigated the effect of the etching on the microstructures by measuring their dimensions. The measurement results are shown in Fig. 10 and indicate that the engraved depth increased with etching time but the width of the concave microstructures changed a little in both case B and case C, thus their aspect ratio also increased as etching time. The microstructures in case B and case C were engraved by the repeatedly horizontally line-scan processing into the round concavities; each round concavity had an outer circular groove around it. The area surrounded by the circular groove was damaged by the laser and thus was easily etched by the HF. In contrast, the area outside the circular groove was not damaged. Therefore, the effect of the etching time on the depth is much higher than that on the width. For case A, the debris was removed, and the surfaces of the pits became smooth. For case B, the debris was removed and the notches of the line-scanning appeared; the notches started to peel when the etching time exceeded 20 min. For case C, the notches started to peel slightly when the etching time exceeded 20 min. Moreover, the microcracks became obvious after being etched in both cases B and C, but did not appear in case A (Fig. 11). Therefore, the point process did not induce the microcracks.

3.4 Effect of HF etching on optical behaviors of glass LGPs

Eight small pieces of samples with array of microstructures engraved can be fabricated on different processing
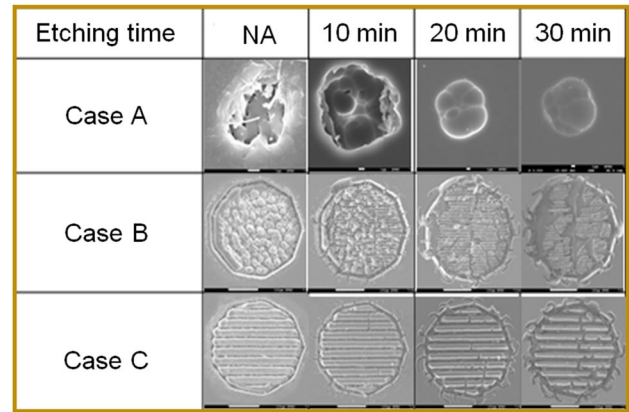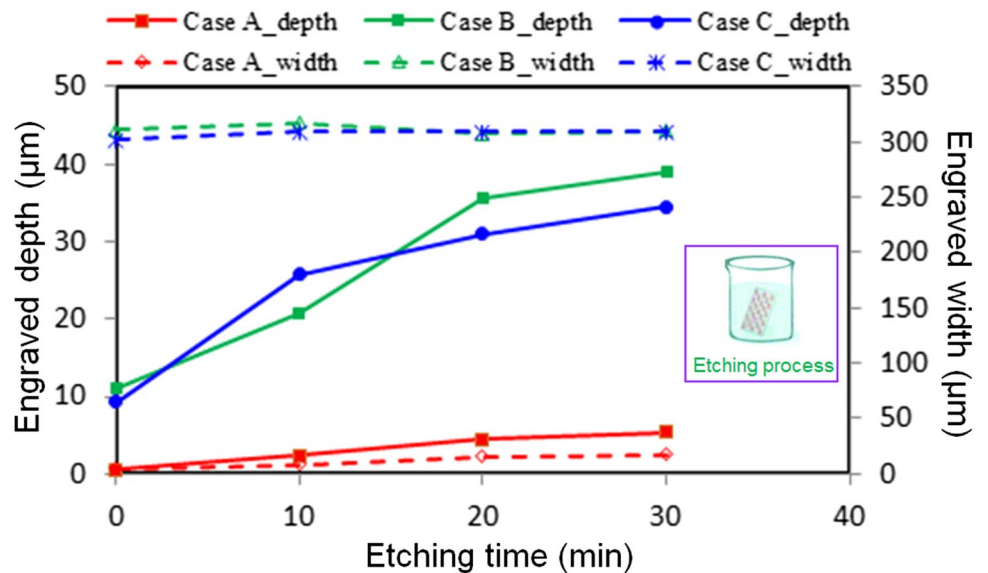

Fig. 11 The appearance of the microstructures varied with etching time

conditions for investigating their optical behaviors before and after they were etched for 5 min. The processing conditions of the eight small pieces of samples were as follows: point processing with engraving time of 0.01 ms, 0.02 ms, 0.03 ms, and 0.04 ms (types 1–4); and line-scan processing with scan pitches of 5 μm, 10 μm, 20 μm, and 30 μm (types 5–8). The dimensions of the samples were 70 mm × 35 mm × 2 mm; the area of the microstructure array was 50 mm × 30 mm, as shown in Fig. 12. We measured the angular intensity and the spatial luminance of light emerging from the samples edge-lit by an LED light-bar to investigate their optical behaviors before and after they were etched. The results about normalized intensity are shown in Fig. 13 and indicate as follows. For the samples engraved by the point processing (types 1–4, Fig. 13(a)), the intensity trends to Lambertian distribution as the engraving time increased because the aspect ratio increased with the

Fig. 10 The effect of the etching time on dimensions of micro-structures

Fig. 12 Small pieces of samples for measuring their optical behaviors
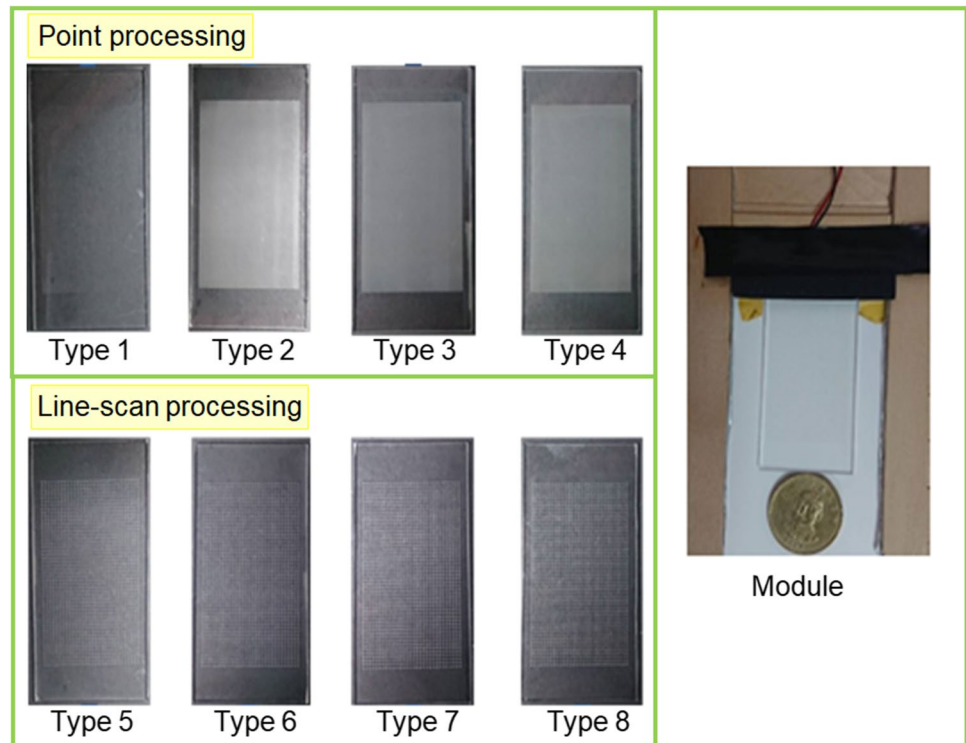

engraving time. Moreover, the crater-like profile and corrugated surface of the microstructure played a role because the light hitting such microstructures diffused further in angles. Therefore, the intensity departs away from Lambertian distribution further after the samples were etched such that the crater-like part was removed and the shallow pits were smoothed. For the samples engraved by the line-scan processing (types 5–8, Fig. 13(b)), the intensity distribution trends to Lambertian distribution for all the samples because the profile of the grooved microstructures with steep slopes made the incident light diffuse intensively in angles. Moreover, the intensity distribution trends closer to Lambertian distribution after the samples were etched. Although the etching smoothing the surface of the microstructures reduced the angularly diffusing of the light, the etching also increasing the depth of the microstructures made the light diffuse further in angles.

The results about spatial luminance are shown in Fig. 14 and indicate as follows. For the samples engraved by the point processing (types 1–4, Fig. 14(a)), the spatial luminance decreased with the distance from the measurement point to the edge-lit LEDs, and the trend became more obvious after the samples were etched. Moreover, the light extracted from the sample with the increase of the engraving time (Type 4 > Type 3 > Types 2 > Type 1) and further rose as the samples after being etched because the aspect ratios of the pits became higher. For the samples engraved by the line-scan processing (types 5–8, Fig. 14(b)), the

spatial luminance also decreased with the distance from the measurement point to the edge-lit LEDs, but the trend kept the same after the samples were etched. Moreover, the light extracted from the sample substantially decreased with the engraving scan-pitch; more light was extracted from the samples after being etched because the microstructures became deeper.

The shape of the concave microstructure has effect on the optical behavior of the light emerging from the LGP. Most of the engraved microstructures are such as the shallow pit, the crater-like concavity, and the trench (or groove). The very shallow pits tend to induce the light to emerge out of the LGP surface in a larger slanted angle with narrower angular distribution; the deeper concavities tend to induce the light to emerge out of the LGP surface in a less slanted angle (i.e., closer to the normal direction) with wider angular distribution. The purpose of the point processing was originally to engrave the glass LGP surface with shallow pits; the purpose of the line-scan processing was originally to engrave the glass LGP surface with deeper circular concavities. However, the experiment results show that the shallow pits on the glass LGP induced the light to emerge out of the LGP surface in an angle not as slanted as expected because the shallow pits on the glass LGP had rough surface leading the light to diffuse widely. Although HF etch made the surface of the shallow pits become smooth, it also made the pits become deeper concavities leading the light to emerge out of the LGP surface with approximately Lambertian distribution

Fig. 13 Normalized intensity of the light emerging from the samples before and after being etched for 5 min: (a) samples of types 1–4; (b) samples of types 5–8


(a)

(b)
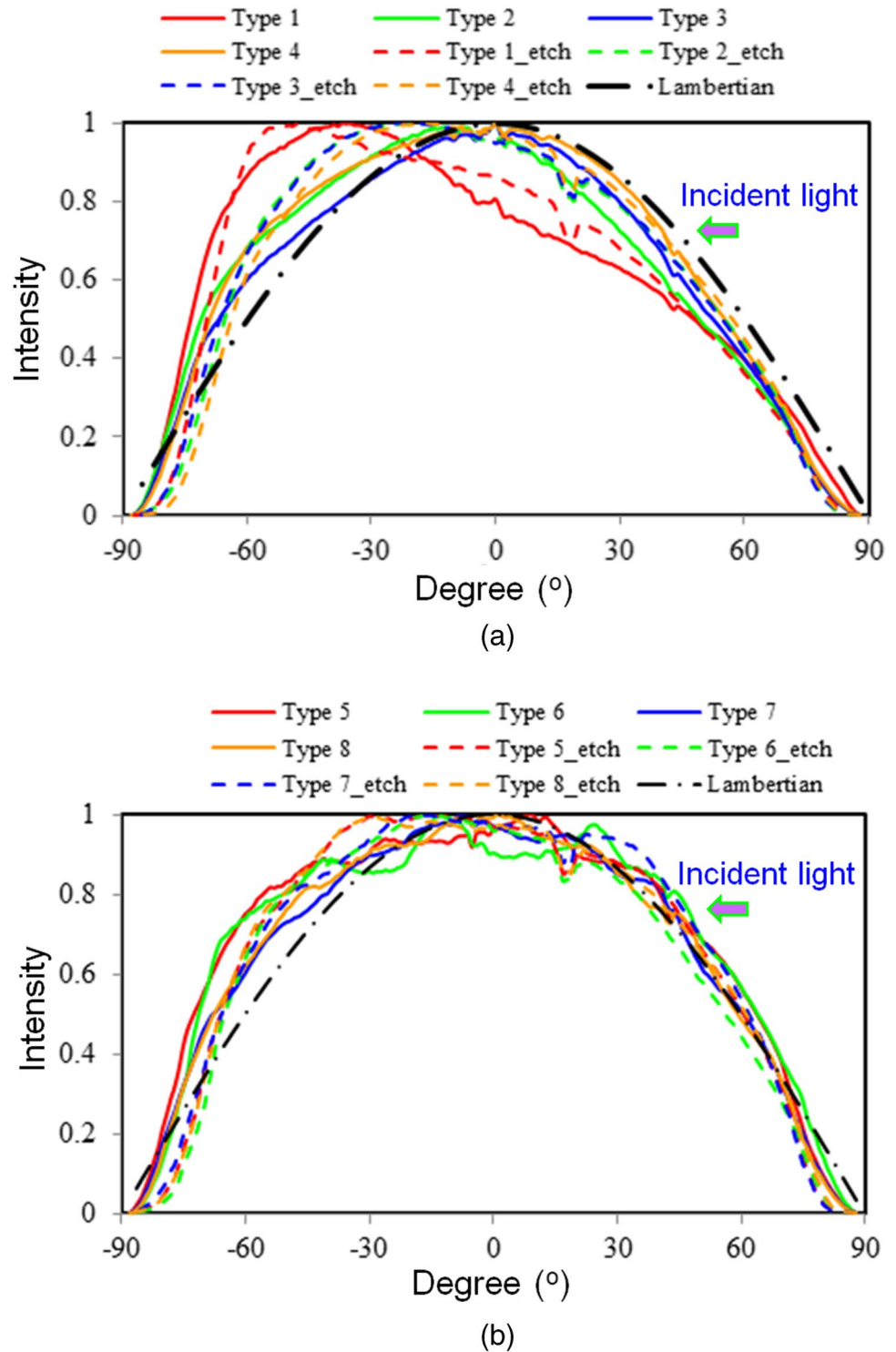
(Fig. 13(a) vs. Figure 13(b)). Therefore, the two kinds of laser processing made the glass LGP have the similar optical characteristic in this study. Considering the processing time and efficiency of light extraction, we engraved two pieces of 6-inch glass LGPs with concave microstructures in 0.3 mm diameter and 0.01 mm scan-pitch by line-scan processing for measuring optical performance.

3.5 Optical performance of a 6-inch glass LGP with engraved microstructures

A 7.8-inch backlight module contained two pieces of 6-inch glass LGPs, and each LGP was edge-lit by an LED light-bar with 24 pieces of LEDs at the input current of 0.2 A as shown in Fig. 15(a). To obtain uniform spatial

Fig. 14 Spatial luminance of the light emerging from the samples before and after being etched for 5 min: (a) samples of types 1–4; (b) samples of types 5–8
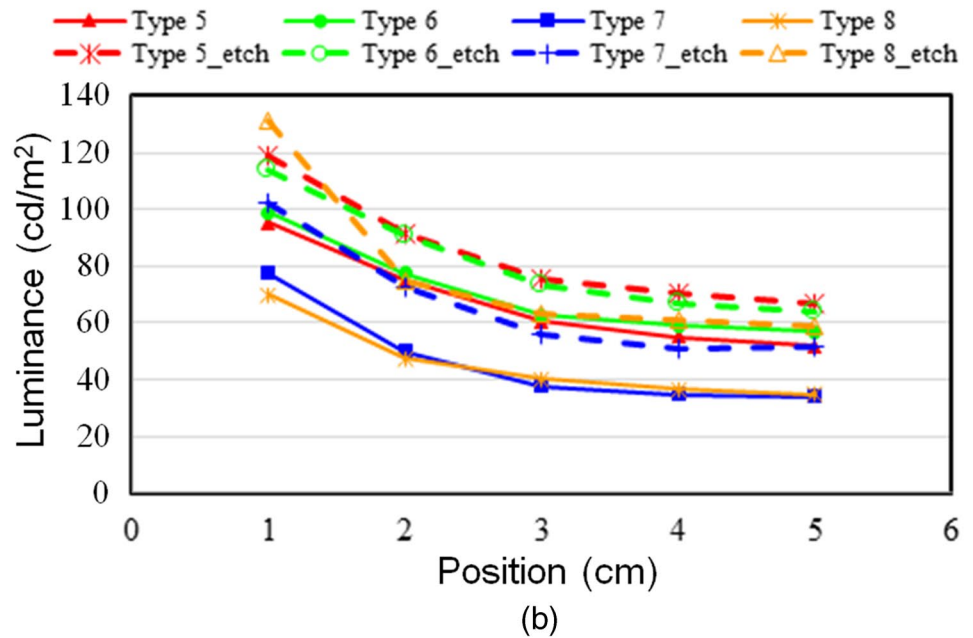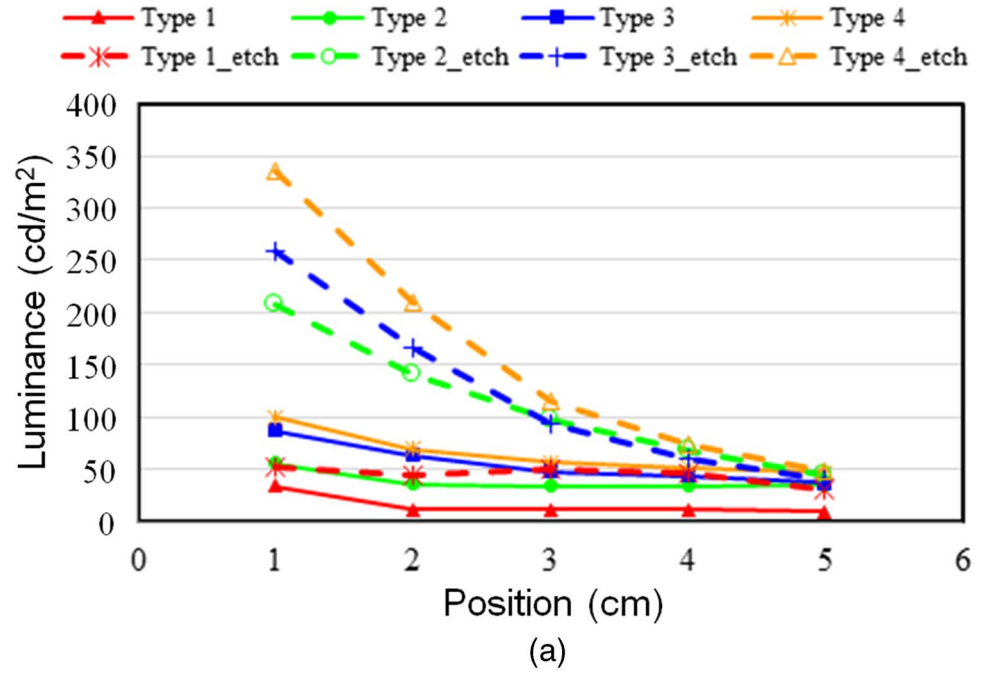
luminance on the backlight module, the microstructures on the LGP surface distributed sparsely in the region near the LEDs, and distributed gradually densely in the region away from the LED. We define the density (ρ) of the microstructures as the ratio of the area of the LGP occupied by microstructures to the area, i.e., the microstructure area ($\sum A_s$) per unit area (A) on the LGP surface. The density distribution was optimized through several trials until the spatial luminance of the backlight was uniform.

The final density distribution on the LGP is as shown in Fig. 15(b), and the density increased from 0.14 up to 0.78. The nine measurement points on the module and their spatial luminance are shown in Fig. 15(c). The W and L were 130 mm and 140 mm, respectively. The measurement results indicate that the average luminance was about 1905 nits and uniformity of the spatial luminance was about 0.87. The definition of the uniformity is the ratio of the minimum to the maximum.
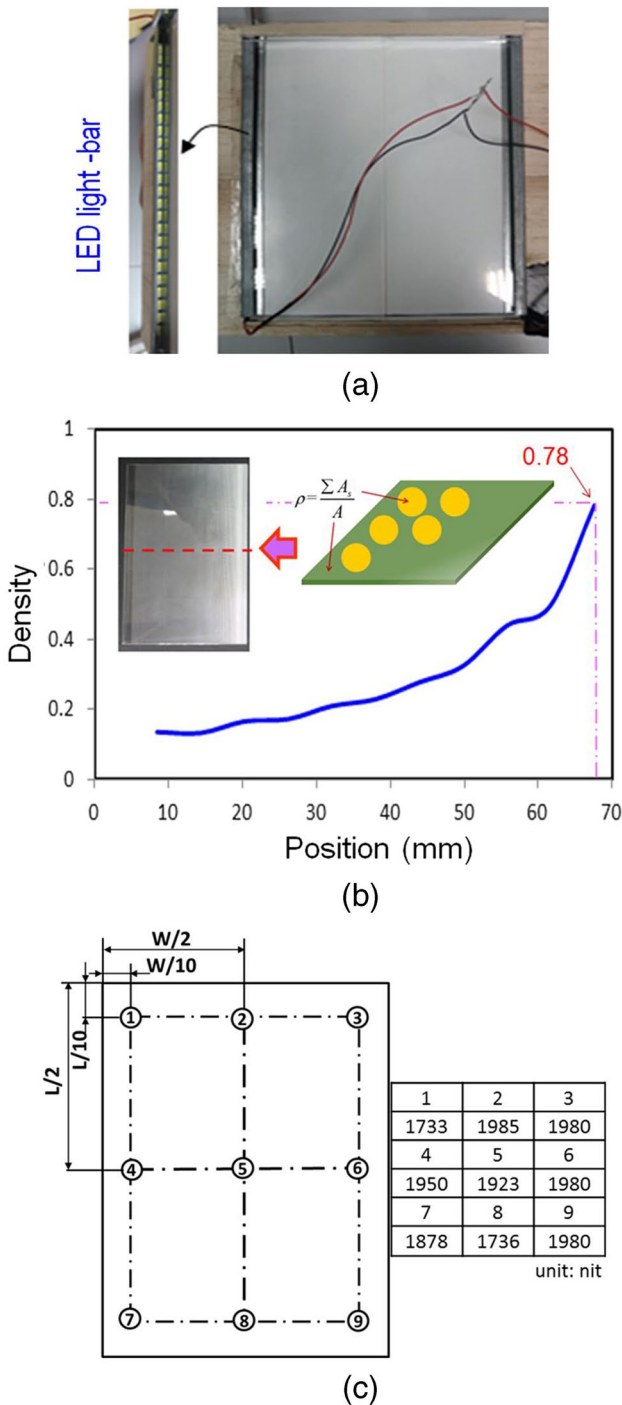
Fig. 15 Spatial luminance of the light emerging from the 7.8-inch backlight module accommodating two pieces of LGP samples: (a) backlight module; (b) density distribution of engraved microstructures on the LGP; (c) spatial luminance of 9 points on the backlight module

(b) density distribution figure with $\rho = \dfrac{\Sigma A_i}{A}$, value 0.78 marked.

(c) table:

1	2	3
1733	1985	1980
4	5	6
1950	1923	1980
7	8	9
1878	1736	1980

unit: nit

with concave microstructures are analyzed. And the microstructures on the LGP can be easily formed through the use of a directly engraved technique with the industrial ability of pico-laser pluses. A process of engraving a 6-inch glass sheet (Corning Iris® Glass) with functional concave microstructures for backlighting was presented, demonstrating particular usefulness for manufacturing glass LGPs in the cases of microstructure-changes in processing methodology. The results indicated three major achievements:

1. The process windows for both the point processing and the line-scan processing were determined. The focal range of the line-scan processing was wider than the point processing; the higher power output provided wider focal range. In addition, the HF etching can smooth the surfaces of the engraved microstructures and removed debris. The aspect ratio of the microstructures that were engraved either by the point processing or the line-scan processing increased with the etching time. The etching results show that the point process can induce the microcracks much less than the line-scan processing.
2. Eight small pieces of glass LGP samples with array of engraved microstructures were made on various processing conditions for measuring the optical characteristic such as angular intensity and the spatial luminance of light emerging from the samples that were edge-lit by an LED light-bar before and after being etched. The intensity departs away from Lambertian distribution further after the samples were etched for the point-processing samples, but trends to Lambertian distribution for the line-scan processing samples. After being etched process, light extraction of the engraved microstructures enhanced.
3. The 6-inch glass LGPs were engraved with concave microstructures in 0.3 mm diameter with 0.01-mm scanning pitch by line-scan processing, in which the distribution of the microstructures on the LGP surface was optimized to make the light exit from the LGP surface uniformly. The two optimized glass LGP samples were put in a 7.8-inch backlight module; the average spatial luminance and the uniformity of the spatial luminance were about 1905 nits and 0.87, respectively.

Therefore, the effects of optical characteristics based on processing strategy could be employed in promoting the application of thinner display products in the manufacturing of LGPs for lighted-up in a BLU.

4 Conclusion

In this study, several types of the optical characteristics on practical verification of laser-engraved glass light guide plate

Declarations

References

1. Chen HW, Lee JH, Lin BY, Chen S, Wu ST (2018) , Liquid crystal display and organic light-emitting diode display: present status and future perspectives. Light: Sci Appl 7:17168
2. Teng TC, Tseng LW (2015) Planar apparatus for uniformly emitting light with angular color-separation. Opt Express 23:A553–A568
3. Teng TC, Sun CH (2020) Integrating backlight with color-filter-free panel for enhancing performance of LCD. IEEE Photonics J 12:7000116
4. Yoon G, Bae S, Lee Y, Yoon J (2018) Edge-lit LCD backlight unit for 2D local dimming. Opt Express 26:20802–20812
5. Yan Z, Du C, Xie Y (2020) Analysis of Low profile head up display using light-guided technology. Optik 203:164056
6. S. Burdette, D. Joshi, A. Tremper, H. Vepakomma (2017) Mechanics of ultra-slim television sets with glass light guide plate, SID 2017 Digest, Japan, 1209–1212
7. K. Hsiao, R. Chien, J. Chang, D. Li, X. Xu (2017) 3.9-mm ultra-slim curved TV having a glass light-guide plate, SID 2017 Digest, Japan, 1205–1208
8. Quesada M, Li S, Senaratne W, Kanungo M, Mi XD, Stempin L, Walczak W, Carleton T, Maurey P, Liu L, Tadesse H, Dabich L (2019) All-glass, lenticular lens light guide plate by mask and etch. Opt Mater Express 9:1180–1190
9. Sekiguchi Y, Kaneko H (2016) Simple ray-tracing model for a rough surface of an ink layer including internal scattering particles printed on a light guide plate. Appl Optics 55(4):908–919
10. Ye ZT, Pai YM, Chen CH, Kuo HC, Chen LC (2019) A light guide plate that uses asymmetric intensity distribution of mini-LEDs for the planar illuminator. Curr Comput-Aided Drug Des 9:141
11. Jang HS, Cho MW, Park DS (2008) Micro dot patterning on the light guide panel using powder blasting. Sensors 8:877–885
12. Tien CH, Hung CH, Yu TH (2009) Microlens arrays by direct-writing inkjet print for LCD BLU applications. J Display Technol 5:147–151
13. Park S, Shin Y, Choi E, Ma H, Lee S (2012) "Improvement of luminance and uniformity of light guide panel using scatterer pattern by laser processing. Opt Laser Technol 44:1301–1306
14. Teng TC (2013) A novel feasible digital laser-blastering to fabricate a light-guide-plate of high luminance and efficiency for TV application. J Display Technology 9:800–806
15. Petrovic J (2019) Durability of the refractive index change induced by a single femtosecond laser pulse in glass. Opt Mater X 1:100004
16. Chang TL, Huang CH, Chou SY, Tseng SF, Lee YW (2017) Direct fabrication of nanofiber scaffolds in pillar-based microfluidic device by using electrospinning and picosecond laser pulses. Microelectron Eng 177:52–58
17. Nouhi A, Spelt JK, Papini M (2018) Abrasive jet turning of glass and PMMA rods and the micro-machining of helical channels. Precision Eng 53:151–162
18. Liu H, Fu Z, Yang K, Xu X, Bauchy M (2019) Machine learning for glass science and engineering: a review. J Non-Cryst Solids: X 4:100036
19. Rodríguez A, Arriola A, Tavera T, Pérez N, Olaizola SM (2012) Enhanced depth control of ultrafast laser micromachining of microchannels in soda-lime glass. Microelectron Eng 98:672–675
20. Delgado T, Nieto D, Flores-Arias MT (2015) Fabrication of microlens arrays on soda-lime glass using a laser direct-write technique and a thermal treatment assisted by a CO_2 laser. Opt Laser Eng 73:1–6
21. Delgado T, Nieto D, Flores-Arias MT (2016) Soda-lime glass microlens arrays fabricated by laser: comparison between a nanosecond and a femtosecond IR pulsed laser. Opt Laser Eng 86:29–37
22. Wang M, Lin JT, Xu YX, Fang ZW, Qiao LL, Liu ZM, Fang W, Cheng Y (2017) Fabrication of high-Q microresonators in dielectric materials using a femtosecond laser: principle and applications. Opt Communications 395:249–260
23. Chen GY, Piantedosi F, Otten D, Kang YQ, Zhang WQ, Zhou X, Monro TM, Lancaster DG (2018) Femtosecond-laser-written microstructured waveguides in BK7 glass. Sci Rep 8:10377
24. Chen ZC, Chang TL, Li CH, Su KW, Liu CC (2019) Thermally stable and uniform DNA amplification with picosecond laser ablated graphene rapid thermal cycling device. Biosens Bioelectron 146:111581
25. Gattass RR, Mazur E (2008) Femtosecond laser micromachining in transparent materials. Nat Photon 2:219–225
26. Chang TL (2013) Micromachining of microfluidic channels in glass by microjoule femtosecond laser pulses. Microelectron Eng 110:450–456
27. Bérubé J, Vallée R (2016) Femtosecond laser direct inscription of surface skimming waveguides in bulk glass. Opt Lett 41:3074–3077
28. Mačernytė L, Skruibis J, Vaičaitis V, Sirutkaitis R, Balachninaitė O (2019) Femtosecond laser micromachining of soda–lime glass in ambient air and under various aqueous solutions. Micromachines 10:354
29. Ito Y, Shinomoto R, Nagato K, Otsu A, Tatsukoshi K, Fukasawa Y, Kizaki T, Sugita N, Mitsuishi M (2018) Mechanisms of damage

formation in glass in the process of femtosecond laser drilling. Appl Phys A 124:181

30. Xu S, Yao C, Dou H, Liao W, Li X, Ding R, Zhang L, Liu LH, Yuan X, Zu X (2017) An investigation on 800 nm femtosecond laser ablation of K9 glass in air and vacuum. Appl Surf Sci 406:91–98

31. Butkus S, Gaižauskas E, Mačernytė L, Jukna V, Paipulas D, Sirutkaitis V (2019) Femtosecond beam transformation effects in water, enabling increased throughput micromachining in transparent materials. Appl Sci 9:2405